Available online at www.sciencedirect.com
SCIENCE DIRECT®
Journal of Solid State Chemistry 177 (2004) 245–250
JOURNAL OF SOLID STATE CHEMISTRY
http://elsevier.com/locate/jssc

Biopolymer immobilization during the crystalline growth of layered double hydroxide

Fabrice Leroux,* Julien Gachon, and Jean-Pierre Besse

Laboratoire des Matériaux Inorganiques, Université Blaise Pascal, UMR 6002, Aubière Cédex 63177, France

Received 27 May 2003; received in revised form 24 July 2003; accepted 1 August 2003

Abstract

Alginic acid, a biopolymer produced by brown seaweed, is incorporated between the sheets of a layered double hydroxide (LDH) via direct coprecipitation. The growth of the inorganic crystalline seeds over the polymer gives rise to a lamellar structure. The obtained nanocomposite presents a basal spacing in agreement with the ideal picture of the polymer lying perpendicularly to the inorganic sheets. A study using FTIR and ^{13}C CP-MAS spectroscopies suggests that the interaction between the organic guest and the inorganic framework is weak. However, the polymer has a stabilizing effect in temperature, since ZnO is observed at 350°C, whereas it appears at 200°C for the chloride LDH pristine material.

Keywords: Layered double hydroxide; Biopolymer; Bio-organoceramic

1. Introduction

Alginate, a heteropolysaccharide having a non-regular structure, has extensively been studied for its property in gel formation [1] and its subsequent application in the food packaging and pharmaceutical industries. Extracted from brown seaweed, the glycuronan is considered as a linear copolymer with alternative sequences of guluronate (G) and mannuronate (M), presenting a (1→4) glycosidic linkage, diaxial or diequatorial, respectively [2].

From a biological perspective, an alginate amino-derivative has recently been studied to promote the cell adhesion and growth [3]. There is also an ever-growing interest in mimicking the biomineralization and in duplicating the living bio-assembly by associating a biopolymer and a mineral, such as polylactide/layered silicate nanocomposites [4,5], system relevant for applications as membrane. Alginate-silica biocomposite was used for enzyme and cell immobilization [6]. For this system, it was found that the morphological features of the composites is dependent on the biopolymer content, alginate intervening both nucleation and seed growth process via electrostatic interaction [7]. Upon the addition, the alginate, which is shaped as a "egg-box", can accommodate divalent cations, such as Co^{II}, Cu^{II} and Mn^{II}, into its cavities via an interaction with its carboxylic groups [8].

We were interested to know how the biopolymer could orientate the assembly of inorganic intricate lamellae such as those of a layered double hydroxide (LDH) $Zn_2Al(OH)_6$ (A) nH_2O. Lamellar LDH structure is commonly described as edge-sharing octahedra sheets in which, by comparison to the brucite $M(OH)_2$, a part of divalent cations is replaced by trivalent cations [9]. The excess of charge, i.e. Al^{3+} content, is counter-balanced by interlayered anions (A), leading to an anionic exchange capacity. The latter impedes usually the intercalation/diffusion of large molecule such as polymer, thus a "templating" method, which consists in the coprecipitation in presence of the polymer, is preferred for LDH [10].

Incorporation of biomolecules into LDH structure [11], such as adenosine monophosphate [12], L-phenylalanine [13], deoxycholic acid [14], DNA [15,16], and biopolymer such as poly(α, β-aspartate) [17], has been reported. For the latter system, it was found that the polyamino acid influenced strongly the cation composition, deviating from an initial ratio of Mg to Al of 2 to

*Corresponding author. Fax: +33-4-734-07-108.
E-mail address: fleroux@chimtp.univ-bpclermont.fr (F. Leroux).

0022-4596/$ - see front matter © 2003 Elsevier Inc. All rights reserved.
doi:10.1016/j.jssc.2003.08.013

1.3, and yielding to non-uniform irregular aggregates. It may be of prime importance since the Zn to Al ratio of 2 was chosen because of its matching between the average charge distance ($a\sqrt{3}$) and the alginate repeating unit size [18].

In this study, we synthesize the "bio-organoceramic" material assembled from the alginate and a LDH structure. The interaction between the guest and the inorganic framework is studied by FTIR and ^{13}C CPMAS spectroscopies, and results concerning the thermal stability are presented.

2. Experimental

2.1. Synthesis of nanocomposite

The preparation of nanomposites was carried out using the "templating" method, as previously reported by Lerner et al. [10]. The amount of biopolymer was optimized to 4 times the content of Al^{3+} cations, defined as the anionic exchange capacity of the clay. Typically, 1.82 g (10^{-2} mol) of alginic acid (MW $\approx$ 150,000 g mol^{-1}, Acros Organics, NJ, USA) was dissolved into 500 mL of a solution of decarbonated water. To this solution, two others were added dropwise, a first containing 0.68 g (5×10^{-3} mol) of $ZnCl_2$ (Acros) and 0.603 g (2.5×10^{-3} mol) of $AlCl_3(H_2O)_6$ (Acros), a second composed of NaOH (1 M). The addition, performed at constant pH of 9 under nitrogen atmosphere and vigorous stirring, was completed after 24 h.

The precipitate was aged in the mother liquid for an additional period of time of 24 h under nitrogen atmosphere to avoid the contamination by carbonate. The product was centrifuged and then washed three times with decarbonated water and dried at 40°C. The final powder was finally grinded.

In order to improve the crystallinity, a hydrothermal treatment was carried out, the solid was placed in a sealed Teflon® tube, and kept at 120°C for 3 days under autogenous pressure. There was no evidence of alginate degradation (no release of odors), the ratio C/Zn obtained from elemental analysis was similar.

Alginate free sample, referred as Zn_2Al/Cl, was prepared as described above, in the same conditions of synthesis and drying.

2.2. Characterization

Elemental analysis (H, C, Zn and Al) for alginate LDH compound was performed at the Vernaison Analysis Center of CNRS using inductive conduction plasma coupled to atomic emission spectroscopy (ICP/AES). In the following, the atomic percents are given in weight, Zn:21.71%, Al:4.25%, C:16.42%, H:3.92%.

Powder X-ray diffraction profiles (PXRD) were obtained with a X'Pert Pro Philips diffractometer using Cu$K\alpha$ radiation and equipped with a HTK16 Anton Paar chamber and a PSD-50m Braun detector (aperture on 2–155° channels). In situ temperature XRD measurements were carried out under air with a temperature holding time of 15 min between each measurement. Scans were performed over the 2θ range from 3° to 70° with a step of 0.0387° and a counting time per step of 20 s.

FTIR spectra were recorded on a Perkin-Elmer 2000 FT spectrometer employing the KBr dilution technique. Thermogravimetric (TG) analyses were performed on a Setaram TGA 92 instrument with a linear heating rate of 5°C/min under air.

$^{13}C(I = \frac{1}{2})$ solid state NMR experiments were performed with a 300 Bruker spectrometer at 75.47 MHz. The experiments were carried out using magic angle spinning (MAS) condition at 10 kHz and a 4 mm diameter size zirconia rotor. ^{13}C spectra obtained by proton-enhanced cross-polarization method (CP) are referenced to the carbonyl of glycine calibrated at 176.03 ppm.

Scanning electron micrographs were recorded with a Cambridge Stereoscan 360 operating at 20 kV (Techinauv, A. S., Aubière, France).

3. Results and discussion

From the chemical analysis, the formula of the nanocomposite, expressed per $(OH)_6$, is $Zn_{2.11}Al(OH)_6(C_6O_5H_7)_{1.45}$ 4.4 H_2O.

The molar ratio Zn/Al is close to the expected value (theoretical of 2, experimental 2.11), indicating that the reaction was complete during the reaction of coprecipitation in presence of the polymer. However, a part of the polymer is located on the surface of the nanocomposite, since the total amount of organics exceeds the Al^{3+} content. It may be explained by some polymer chains embedding the crystallites, as visualized on the SEM micrographs (vide infra). It is usually observed for such lamellar systems exhibiting strong adsorption properties [19].

3.1. Incorporation of organic

The material Zn_2Al/Cl is well crystallized as observed by the X-ray diffraction pattern (Fig. 1a). Diffraction peaks are typical of the LDH structure [18]. The reflections were indexed in a hexagonal lattice with a *R*-3*m* rhombohedral symmetry.

The incorporation of the biopolymer between the layers is confirmed by an increase in the basal spacing from 7.79 to 13.04 Å (Fig. 1b). This value is the sum of the inorganic layer thickness, which is estimated to 4.8 Å

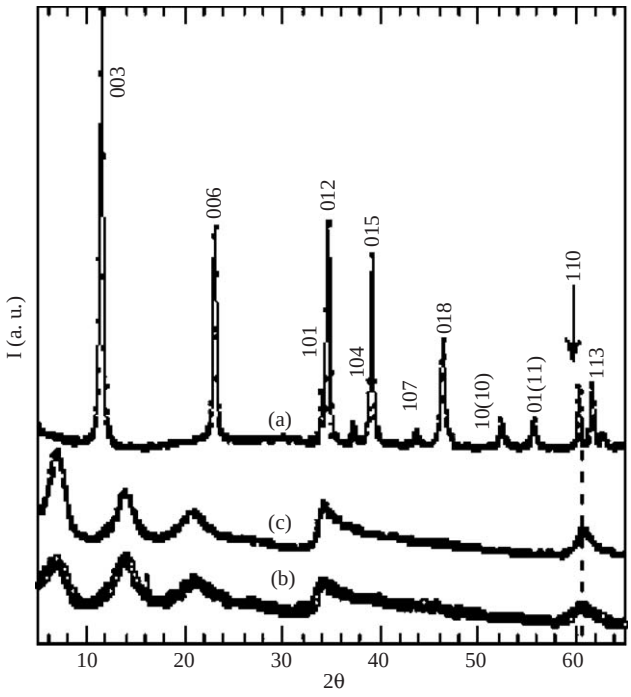

Fig. 1. X-ray diffraction patterns of (a) Zn_2Al/Cl and of Zn_2Al/alginate (b) as prepared and (c) after hydrothermal treatment. Miller indexation is given in the diagram for Zn_2Al/Cl.

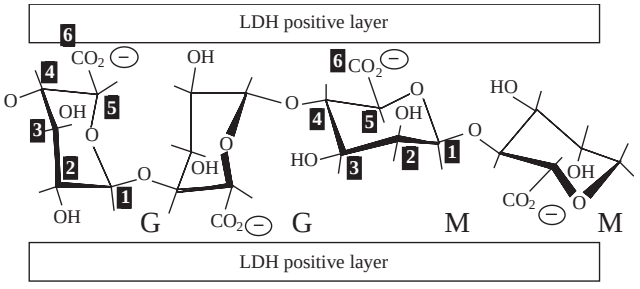

Fig. 2. Proposed structural arrangement of the "bio-assisted" nanocomposite Zn_2Al/alginate. For clarity, the two conformations of alginate, guluronate (G) and mannuronate (M), are shown.

in comparison to the brucite, and of the interlayer distance, which is the space available for the accommodation of the alginate. The dimension of the interlamellar gap (≈ 8 Å) is consistent with the presence of the polymer lying more or less perpendicularly to the sheets. Alginate is considered as a linear copolymer alternating in an intricate way G and M repeating units [2]. An ideal model of its entrapment between the inorganic layers is proposed in Fig. 2.

Since the as-made alginate templated LDH material present ill-defined peaks of diffraction, a subsequent hydrothermal treatment was used to cure the sample. This treatment improves slightly the crystallinity (Fig. 1c). The width of the diffraction peak (00l) is lowered, it is explained by a greater number of stacked layers or by a decrease of the initial disorder due to turbostatic phenomena. The basal spacing is slightly shifted down to 12.75 Å.

It is noteworthy that any attempt to prepare the nanocomposite by exchange reaction from the chloride LDH phase has failed.

The nanocomposite does not present the usual "sand-rose" morphology of the inorganic LDH parent. The assembly between the biopolymer and the inorganic matrix gives rise to an intricate morphology (Fig. 8), however, the stacked layers are observed (inset of Fig. 3a). The synthesis of LDH oriented by the biopolymer leads to unusual submicronic features, as exemplified in Fig. 8b with the observation of a tubular shape in comparison to the sand-rose morphology of the chloride LDH phase (Fig. 3).

3.2. Interaction between the biopolymer and LDH sheets

IR spectra are displayed in Fig. 4. By comparison to the spectrum of the alginate alone, the presence of the biopolymer is confirmed in the nanocomposite by the different vibration bands, the stretching of the bond (COO^-) located at 1608 and 1413 cm^{-1} and of C–O at 1317 and 1087 cm^{-1}. Additional vibrations are observed, such as the stretching CH and C–O at 2930 and 947 cm^{-1}, respectively. A complete study of the alginate IR spectrum was previously carried out [20,21].

The inorganic lattice vibration appears in the range 400–800 cm^{-1} (Fig. 4a). The vibration bands of COO^-, which represents the anionic group, remain at the same position in the nanocomposite. This shows that there is no strong interaction between the organic guest and the inner surface of the LDH material, in contrast to what was observed with divalent cations such as Co^{2+} in the case of sol–gel transition of the alginate [8].

This is also evidenced by the ^{13}C NMR CP-MAS study. Fig. 5 shows the spectra for the alginate and the nanocomposite. The resonance peaks are assigned according to the literature [2], the nature of the carbon atoms is referred to Fig. 2. A large hump centered at 75–70 ppm is split into closely spaced contributions. They are assigned to the partition between both repeating units, G or M, in the glycuronan (Fig. 5). Even if ^{13}C CP is not a quantitative analysis, from the comparison of both spectra, we can surmise that the polymer conformation is not modified once immobilized between the inorganic layers.

In addition to this, the similarity between both spectra suggests that the alginate does not encounter any shielding effect when incorporated between the sheets of Zn_2Al. Indeed, an interaction with the layers should induce a shielding of the carbon atom COO^-, generally arising from the electrostatic forces between the negatively charged function of the guest and the positively charged layers [22]. These results are

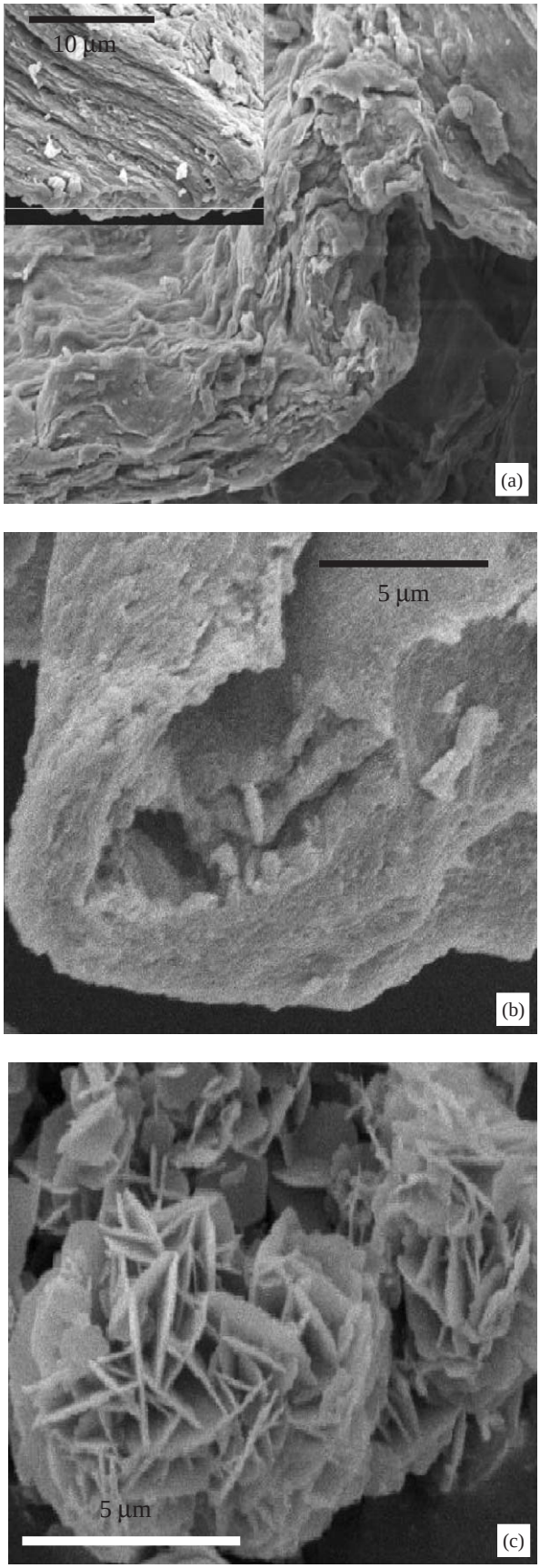

Fig. 3. SEM micrographs of (a) and (b) the nanocomposite Zn_2Al/alginate at different magnitudes and (c) Zn_2Al/Cl.

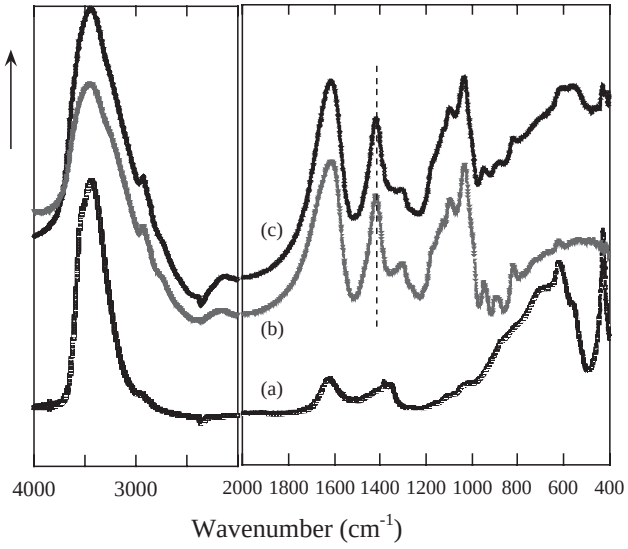

Fig. 4. FTIR spectra of (a) Zn_2Al/Cl, (b) alginate and (c) Zn_2Al/alginate.

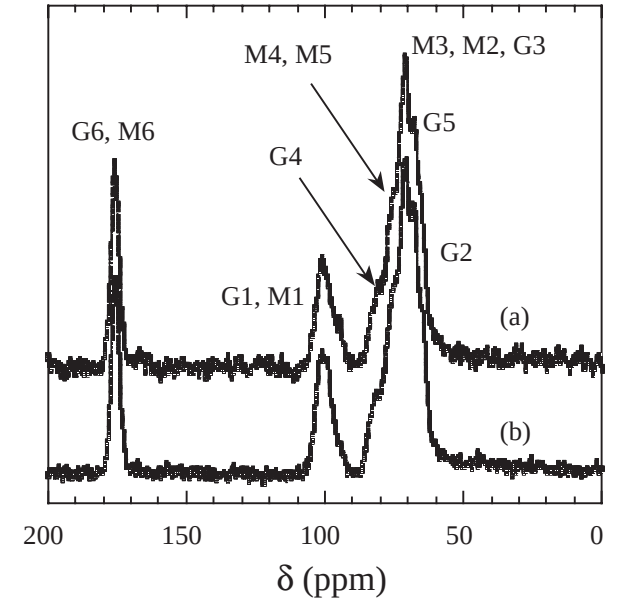

Fig. 5. ^{13}C NMR CP-MAS spectra of (a) alginate and (b) Zn_2Al/alginate. The assignments are given according to Fig. 2.

substantially different from those obtained in the case of divalent cations [8], which were binding in a chelating way through the carboxylic group of the alginate. In our case, this may be explained by the relative stiffness of the inorganic layers [23].

3.3. Stability in temperature

In situ XRD experiments were carried out (Fig. 6). The harmonics (00l) are observed below a temperature of 260°C, showing that the lamellar structure is preserved. However, for a narrow temperature range

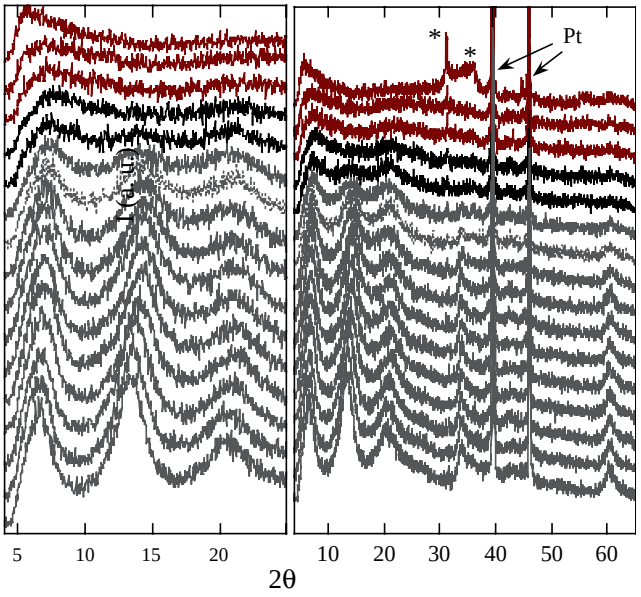

Fig. 6. In situ XRD in temperature of the nanocomposite Zn_2Al/alginate. *represents ZnO. From bottom ($T = 20°C$) to top (320°C), the diagrams are displayed every 20°C.

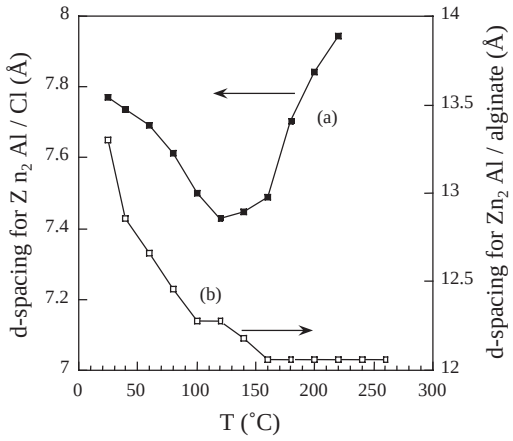

Fig. 7. Variation of the basal spacing vs. T for (a) Zn_2Al/Cl, and (b) Zn_2Al/alginate.

($260 > T > 220°C$), the diffraction peak (110), relative to the intralayer cation local order, is not observed anymore.

Like other polymer/LDH-type systems [24,25], it means that the whole structure can be maintained in spite of the loss of intralayer order. Above 280°C, the degradation of the phase occurs with the observation of ZnO (Fig. 6).

Though not strongly attached to the inorganic layers, the biopolymer stabilizes the lamellar structure, in a greater manner than that exhibited by the chloride pristine LDH material (Fig. 7). For the latter sample, the lamellar structure collapses above 200°C. The decrease in d-spacing is attributed to the dehydration process, whereas its increase concerning the chloride phase was ascribed to a structural rearrangement [24]. Upon calcination, a change from *Oh* to *Td* for the Al coordination is observed, and a possible migration of four-fold coordinated Al atoms may be considered to explain the variation of the basal spacing [26].

3.4. Thermal behavior

Decomposition of the chloride LDH phase proceeds in several weight loss processes (Fig. 8). From room temperature to 200°C, the weight loss is ascribed to the departure of the physisorbed and interlamellar water molecules, the second process arising up to 300°C corresponds to the deshydroxylation, the final weight loss between 500°C and 700°C is due to the departure of the anions [27]. The degradation of the biopolymer occurs in two steps 240°C and 600°C. When the biopolymer is present between Zn_2Al LDH sheets, the first process is delayed, and is concomitant with the dehydration and deshydroxylation of the inorganic layers. The presence of the latter surrounding the polymer stabilizes the assembly in the low temperature range. In contrary, the second process occurs at lower temperature for the nanocomposite than for the polymer, it may be explained by the combustion of the organic residues favored by the presence of the oxide by-products arising from the degradation of the LDH moiety at this temperature. The total weight loss is in good agreement with the chemical formula according to the following equation:

$$Zn_{2.11}Al(OH)_6(C_6O_5H_7)_{1.45}4.4H_2O \rightarrow \text{“}Zn_{2.11}AlO_{3.61}\text{”},$$

$(\Delta m/m)_{exp}$ at 1000°C of 62% has to be compared to $(\Delta m/m)_{th}$ of 61.5%.

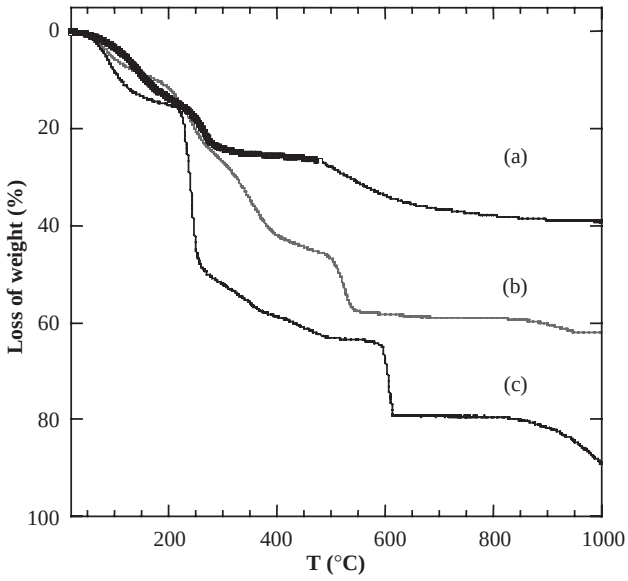

Fig. 8. TG analysis of (a) Zn_2Al/Cl, (b) Zn_2Al/alginate nanocomposite and (c) alginate.

4. Conclusion

This paper shows that LDH lamellar structure can be built from a templating reaction involving an intricate biopolymer such as alginate. Largely employed to incorporate large molecules, the coprecipitation reaction can be extended to biopolymer opening new routes of synthesis for nanocomposites based on LDH-like structure.

Acknowledgments

The authors would like to thank M. Joël Cellier for his help in acquiring the in situ XRD patterns in temperature.

References

[1] X. Liu, L. Qian, T. Shu, Z. Tong, Polymer 44 (2003) 407.
[2] H. Grasdalen, B. Larsen, O. Smidsrod, Carbohydr. Res. 89 (1981) 179.
[3] H. Zhu, J. Ji, R. Lin, C. Gao, L. Feng, J. Shen, Biomaterials 23 (2002) 3141.
[4] P. Maiti, K. Yamada, M. Okamoto, K. Ueda, K. Okamoto, Chem. Mater. 14 (2002) 4654.
[5] M.A. Paul, M. Alexandre, P. Degée, C. Henrist, A. Rulmont, P. Dubois, Polymer 44 (2003) 443.
[6] T. Coradin, E. Mercey, L. Lisnard, J. Livage, Chem. Commun. (2001) 2496.
[7] T. Coradin, J. Livage, J. Sol–Gel Sci. Technol. 26 (2003) 1165.
[8] Z.Y. Wang, Q.Z. Zhang, M. Konno, S. Saito, Biopolymers 33 (1993) 703.
[9] G.W. Brindley, S. Kikkawa, Am. Miner. 64 (1979) 836.
[10] C.O. Oriakhi, I.V. Farr, M.M. Lerner, J. Mater. Chem. 6 (1996) 103.
[11] A.I. Khan, D. O'Hare, J. Mater. Chem. 12 (2002) 3191.
[12] J.H. Choy, S.Y. Kwak, J.S. Park, Y.J. Jeong, J. Mater. Chem. 11 (2001) 1671.
[13] A. Fudala, I. Palinko, I. Kiricsi, Inorg. Chem. 38 (1999) 4653.
[14] M. Ogawa, S. Asai, Chem. Mater. 12 (2000) 3253.
[15] J.H. Choy, S.Y. Kwak, Y.J. Jeong, J.S. Park, Angew. Chem. Int. Ed. 39 (2000) 4042.
[16] J.H. Choy, S.Y. Kwak, J.S. Park, Y.J. Jeong, J. Portier, J. Am. Chem. Soc. 121 (1999) 1399.
[17] N.T. Whilton, P.J. Vickers, S. Mann, J. Mater. Chem. 7 (1997) 1623.
[18] W. Hofmeister, H. von Platen, Cryst. Rev. 3 (1992) 3.
[19] M. El Moujahid, J. Inacio, J.-P. Besse, F. Leroux, Microporous Mesoporous Mater. 57 (2003) 37.
[20] C. Sartori, D.S. Finch, B. Ralph, K. Gilding, Polymer 38 (1997) 43.
[21] N.P. Chandia, B. Matsuhiro, A.E. Vasquez, Carbohydr. Polym. 46 (2001) 81.
[22] M. El Moujahid, J.-P. Besse, F. Leroux, J. Mater. Chem. 12 (2002) 3324.
[23] S.A. Solin, D. Hines, S.K. Yun, T.J. Pinnavaia, M.F. Thorpe, J. Non-Cryst. Solids 182 (1995) 212.
[24] M. El Moujahid, J.-P. Besse, F. Leroux, J. Mater. Chem. 13 (2003) 258.
[25] P.B. Messersmith, S.I. Stupp, Chem. Mater. 7 (1995) 454.
[26] J. Rocha, M. del Arco, V. Rives, M.A. Ulibarri, J. Mater. Chem. 9 (1999) 2499.
[27] F. Leroux, M. Adachi-Pagano, M. Intissar, S. Chauvière, C. Forano, J.-P. Besse, J. Mater. Chem. 11 (2001) 105.